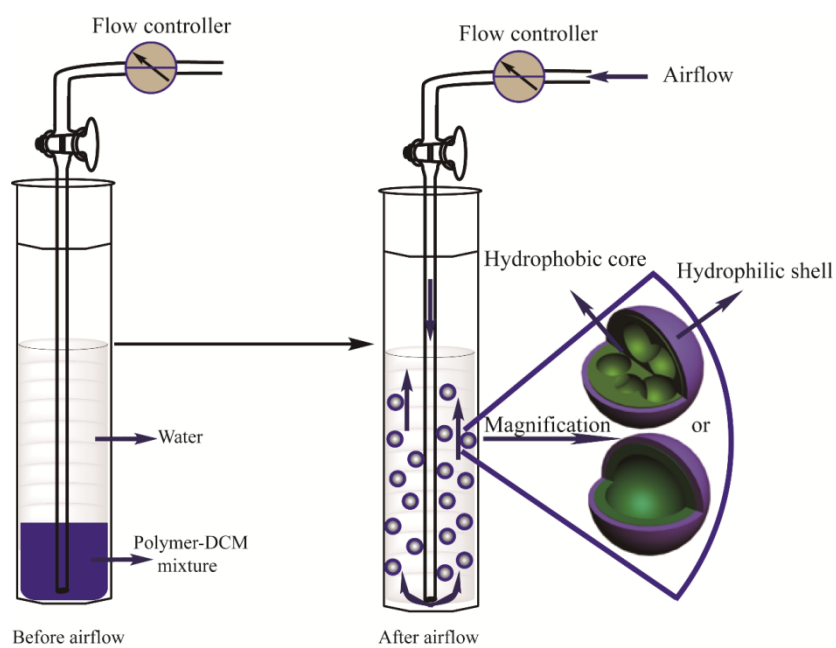


## Supplementary Information

### An airflow-controlled solvent evaporation route to hollow microspheres and colloidosomes

Conghui Yuan <sup>a</sup>, Birong Zeng <sup>a</sup>, Shirong Yu <sup>a</sup>, Jie Mao <sup>a</sup>, Xiaoling Chen <sup>b\*</sup>, Weiang Luo <sup>a</sup>, Yiting Xu <sup>a</sup>,  
Feng-Chih Chang <sup>c</sup>, Lizong Dai <sup>a\*</sup>



Scheme 1S. Formation process of hollow or porous microspheres

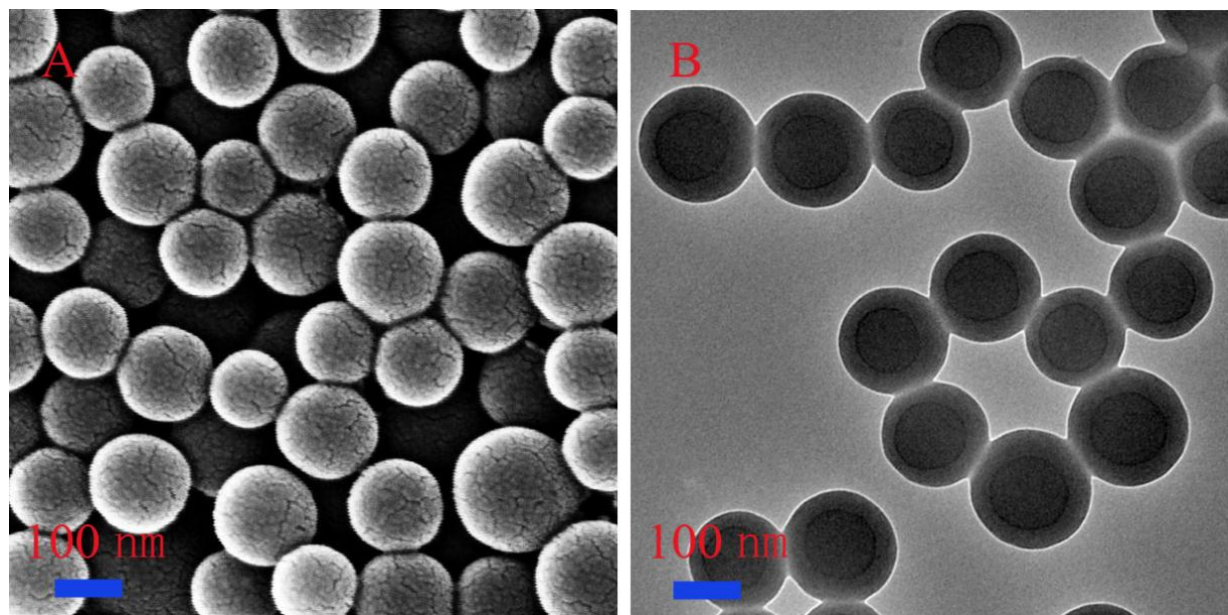


Fig. 1S SEM (A) and TEM (B) images of uncrosslinked P(St-co-O-B-EG600) core-shell nanospheres.

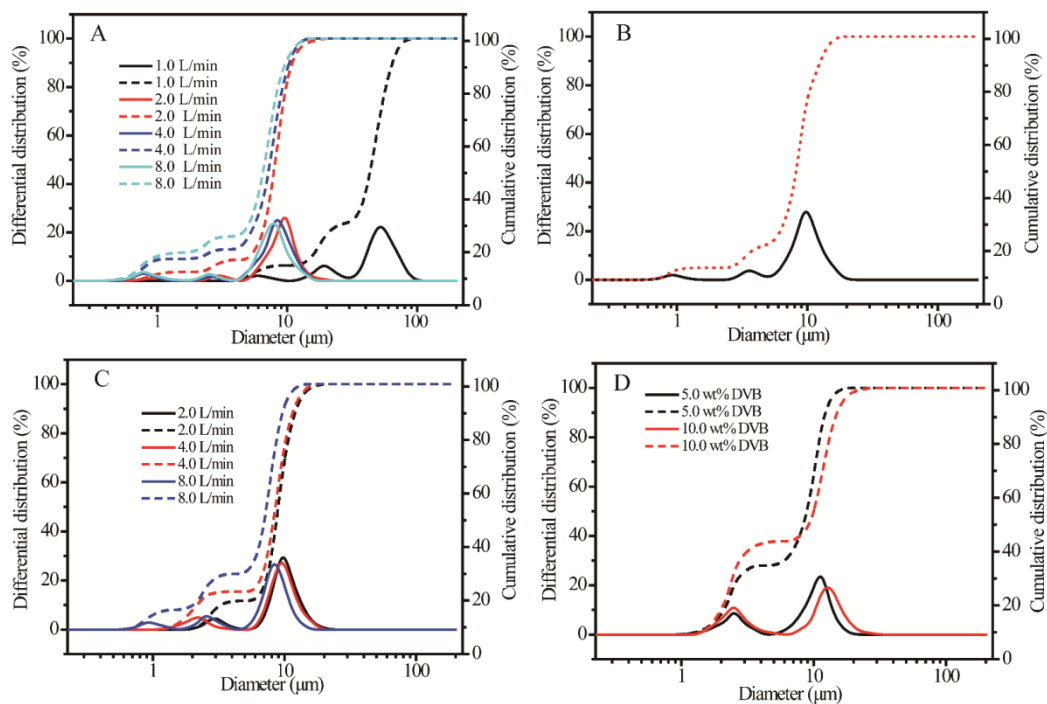


Fig. 2S Diameters of the microspheres, colloidosomes and hybrid colloidosomes, differential distributions (solid lines), cumulative distributions (dash lines). (A) P(St-co-O-B-EG600) microspheres prepared from 1.0, 2.0, 4.0 and 8.0 L/min airflow rates; (B) polymer-polymer nanosphere colloidosomes prepared by using 4.0 L/min airflow rate; (C) polymer-Fe<sub>3</sub>O<sub>4</sub> nanoparticle hybrid colloidosomes obtained from 2.0, 4.0 and 8.0 L/min airflow rates; (D) polymer-polymer nanosphere-Fe<sub>3</sub>O<sub>4</sub> nanoparticle ternary hybrid colloidosomes prepared by using core-crosslinked P(St-co-O-B-EG600) nanoparticles with 5.0 and 10.0 wt% of DVB.

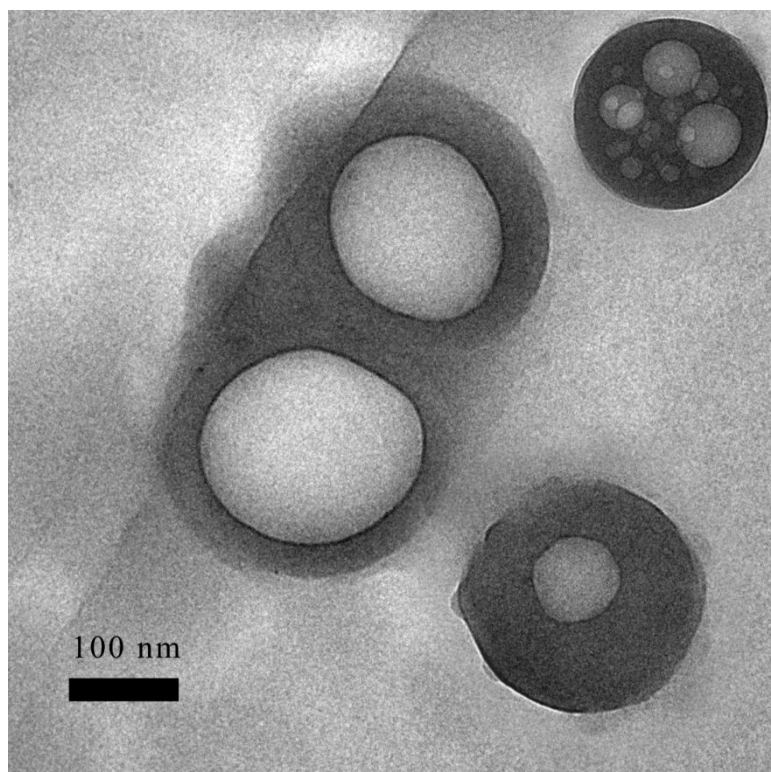


Fig 3S. Typical TEM image of shell-crosslinked P(St-co-O-B-EG600) nanospheres dispersed in DCM.

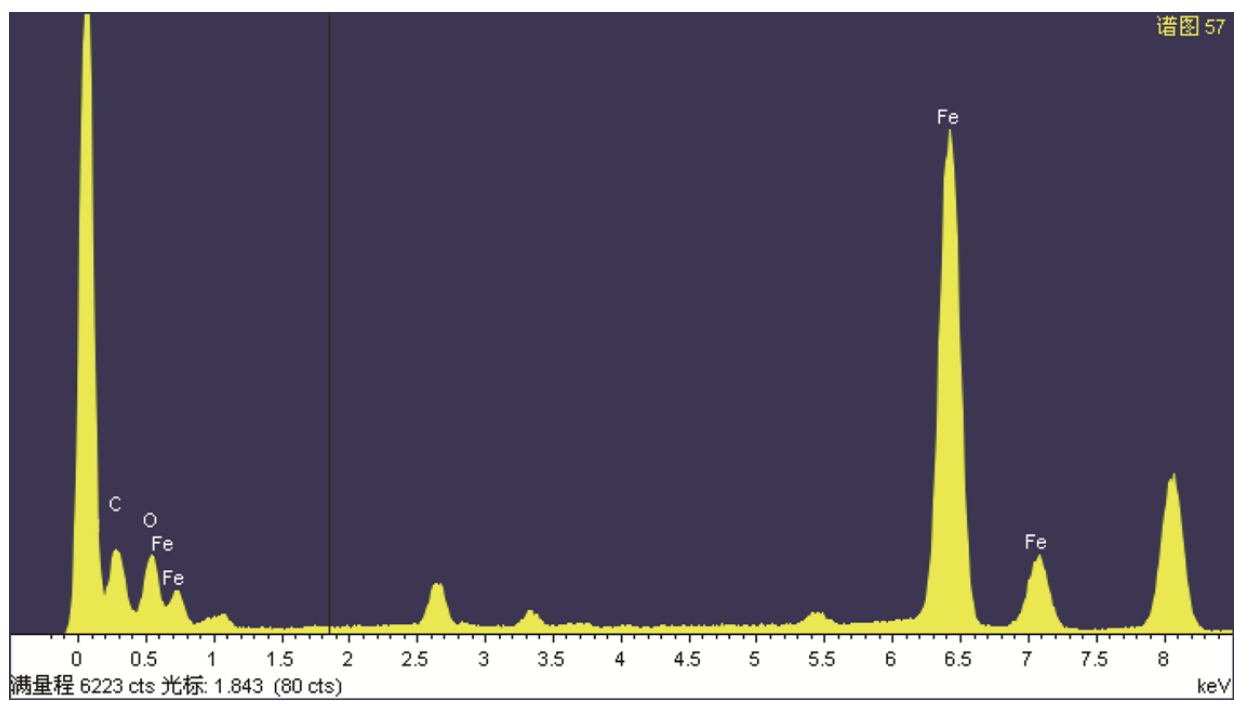


Fig. 4S XPS spectrum of polymer-Fe<sub>3</sub>O<sub>4</sub> nanoparticle hybrid colloidosomes.

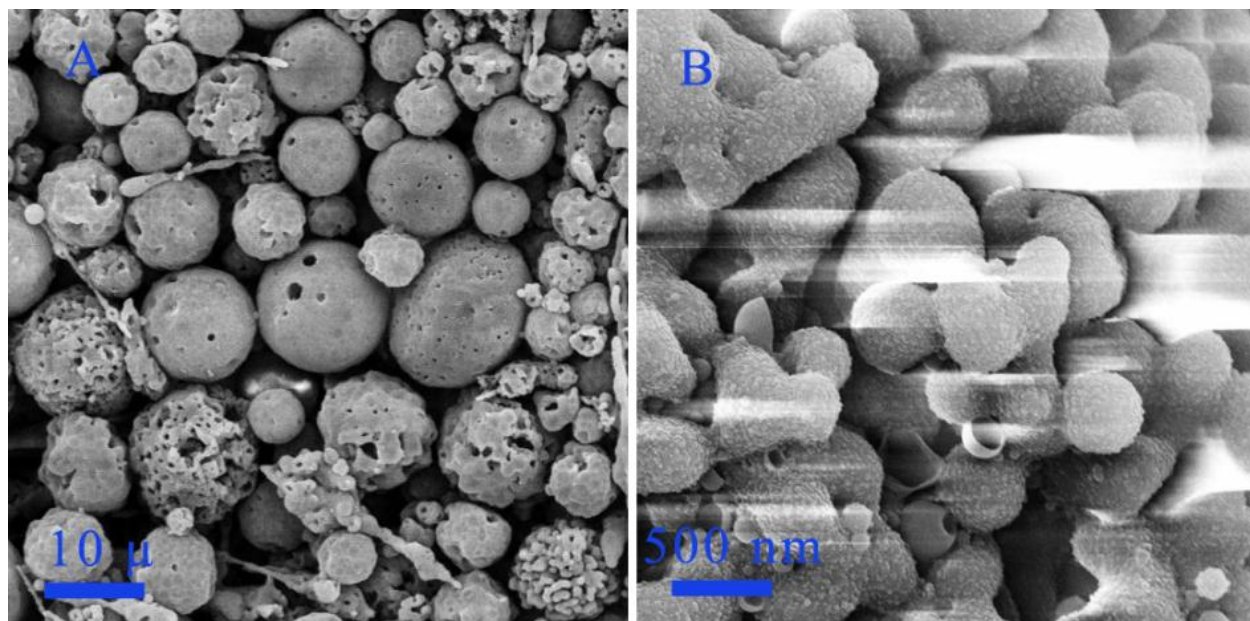


Fig. 5S Overview (A) and magnified (B) SEM images of ternary hybrid colloidosomes prepared by shell crosslinked P(St-co-O-B-EG600) nanospheres.

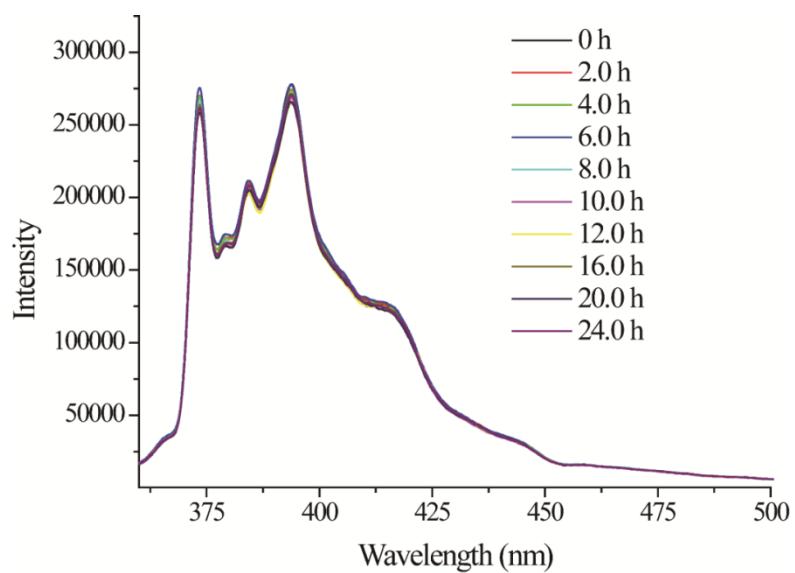


Fig. 6S Fluorescence emission spectra evolution of pyrene encapsulated in ternary hybrid colloidosomes in aqueous solution at room temperature.



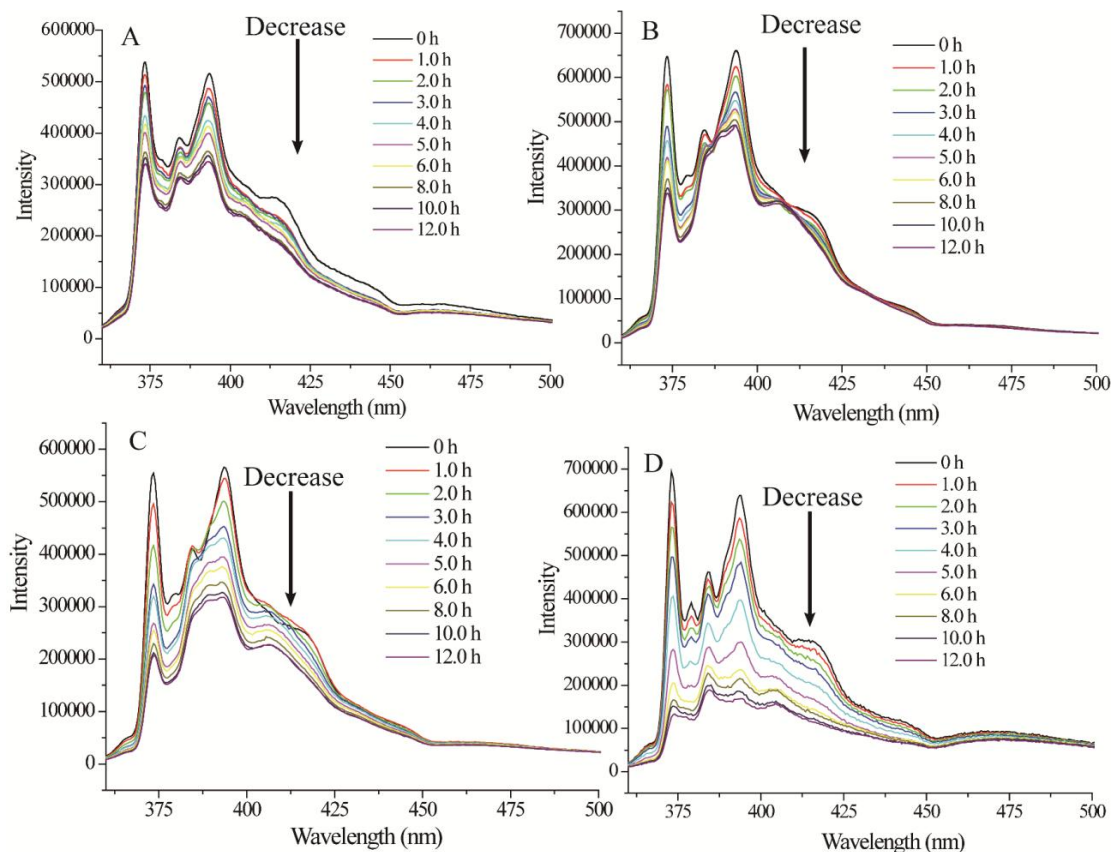


Fig. 7S Fluorescence emission spectra evolution of pyrene encapsulated in hybrid colloidosomes at temperatures 41 (A) and 43 °C (C), and encapsulated in ternary hybrid colloidosomes at temperatures 41 (C) and 43 °C (D) in aqueous solution. Hybrid colloidosomes were generated from 8.0 L/min of airflow, ternary hybrid colloidosomes prepared from P(St-co-O-B-EG600) nanoparticles crosslinked with 10.0 wt% DVB (airflow rate 4.0 L/min).



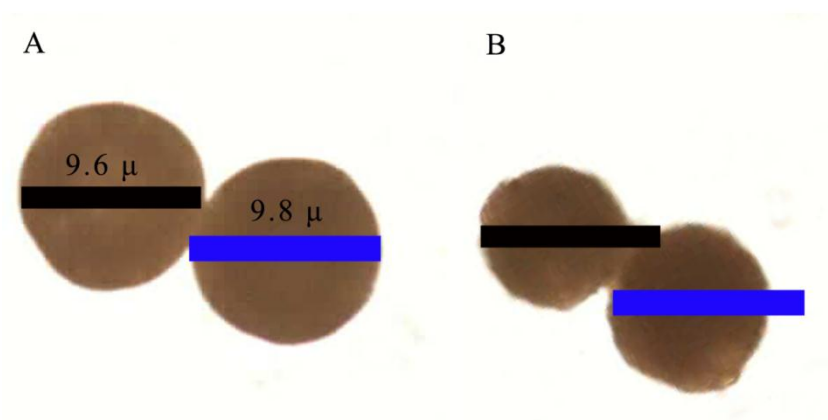


Fig. 8S Optical pictures of hybrid colloidosomes before (A) and after (B) the release of pyrene.

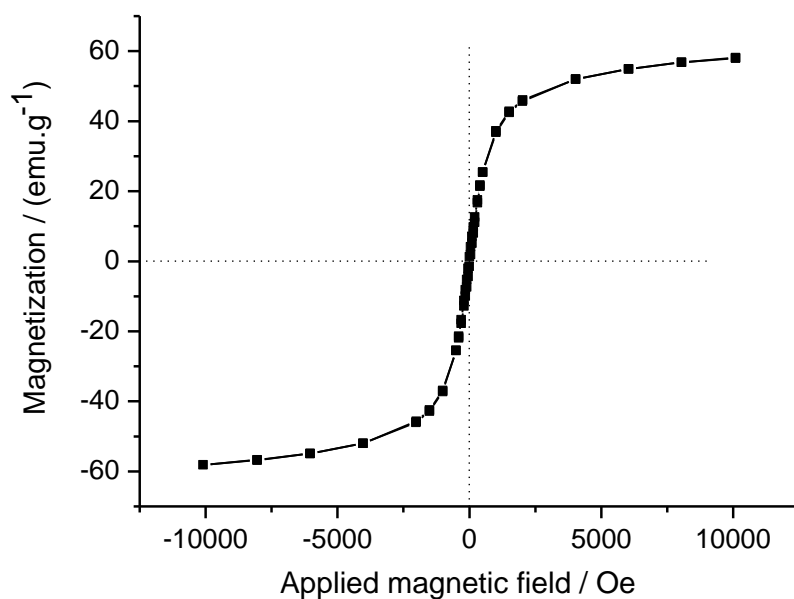


Fig. 9S Magnetic hysteresis loops of OA coated  $\text{Fe}_3\text{O}_4$  nanoparticles.

Table 1S. Feeding contents of  $\text{Fe}_3\text{O}_4$  and actual magnetite contents of hybrid colloidosomes and ternary hybrid colloidosomes

Samples	Airflow (L/min)	DVB crosslinker (%)	Feeding content of $\text{Fe}_3\text{O}_4$ (%)	Actual magnetite content (%)
Hybrid Colloidosomes	2.0	0	15.0	4.2
	4.0	0	15.0	5.7
	8.0	0	15.0	7.0
Ternary hybrid colloidosomes	4.0	5.0	15.0	6.2
	4.0	10.0	15.0	11.7